

See discussions, stats, and author profiles for this publication at: <https://www.researchgate.net/publication/3850152>

Linear induction motor parameter determination on force development applications

Conference Paper · February 2000

DOI: 10.1109/PESW.2000.849989 · Source: IEEE Xplore

CITATIONS

12

READS

290

3 authors, including:



[José Roberto Camacho](#)

Universidade Federal de Uberlândia (UFU)

181 PUBLICATIONS 512 CITATIONS

[SEE PROFILE](#)

Some of the authors of this publication are also working on these related projects:



Electrical Machines [View project](#)



Analysis in the Parameterization of the Inductances and Resistance of the Rotor of a Three Phase Induction Motor using Finite Elements Method [View project](#)

LINEAR INDUCTION MOTOR PARAMETER DETERMINATION ON FORCE DEVELOPMENT APPLICATIONS

Luciano Martins Neto, Dr* Euler B. dos Santos, MSc** José R. Camacho, PhD*

*Universidade Federal de Uberlândia, Depto Engenharia Elétrica
UFU/DEENE/LabMaq

P.O.Box: 593 - Campus Santa Mônica
38400-902 - Uberlândia - MG - Brasil
e.mail: jrcamacho@ufu.br

**Universidade Federal de Goiás, Escola de Engenharia Elétrica
74605-020 - Goiânia - GO - Brasil

Abstract - The main goal in this paper is to present a linear induction motor parameter determination method when its destination is mainly the thrust development. This method is developed basically from the equivalence between the Linear Induction Motor (LIM) and the ordinary asymmetrical induction motor. In this case it is used the theory of symmetrical and asymmetrical components of positive, negative and zero sequence. Experimental procedures with the LIM prototype can support the theoretical and experimental validation for this method.

Index terms - linear induction motor, force, parameter determination.

I. INTRODUCTION

The purpose of this work is to develop a methodology to obtain the parameters for the LIM based on its equivalence with the asymmetrical rotary induction motor. The asymmetrical motor considered in this case is an ordinary three-phase rotary induction motor with a cylindrical squirrel cage rotor and with the stator phases having different turns number. Therefore can be taken by abstraction a rotary asymmetrical motor which has equivalent characteristics to the mentioned LIM, taking in consideration its electrical and mechanical terminals. In this sense, all the modeling is developed taking into consideration the rotary asymmetrical induction motor model. The idea of equivalence was brought by the fact of the LIM design asymmetry and the availability of the asymmetrical induction motor model, making the proposed method a real possibility.

II. MATHEMATICAL MODEL

A LIM when fed by a sinusoidal three-phase balanced line voltage system presents in its terminal currents and voltages which are not balanced. This happens due to the design aspects and end effects.

To the rotary asymmetrical induction motor the voltage equation in one generic phase η ($= a, b, c$) in the primary can be written as follows:

$$\dot{V}_{\eta} = \dot{Z}_{\eta} \dot{I}_{\eta} + \dot{E}_{\eta} \quad (1)$$

where:

\dot{V}_{η} - voltage vector in a generic primary phase η ;

\dot{Z}_{η} - impedance, a representation of primary winding leakage reactance and resistance, for the generic phase η ;

\dot{I}_{η} - current vector for the primary generic phase η ;

\dot{E}_{η} - primary winding electromotive force(emf). for the generic phase η .

Taking into consideration the phase sequence as being ABC and phase A as the reference, and the machine speed is in agreement with this sequence, the unbalanced feeding current system can be decomposed in its symmetrical components. Knowing that the primary winding is Y connected with floating neutral, the current positive (\dot{I}_{a1}), negative (\dot{I}_{a2}) and zero (\dot{I}_{a0}) sequence components[2] can be obtained, with the unbalance degree (\dot{f}_d) given by:

$$\dot{f}_d = \frac{\dot{I}_{a2}}{\dot{I}_{a1}} \quad (2)$$

The air-gap magneto-motrice force (mmf) space harmonics will establish magnetic field with identical harmonic spectrum, which will be responsible for the existence of induced voltages in the primary winding.

The induced voltages referred to the h^{th} space field harmonic will have only positive $\dot{E}_{aph}, \dot{E}_{bph}, \dot{E}_{cph}$ and negative $\dot{E}_{anh}, \dot{E}_{bnh}, \dot{E}_{cnh}$ sequence components [7].

Through Faraday's Law and having the "A" phase as a reference the relationship among these components of induced voltages are related by the following equations :

$$b \dot{E}_{bph} = a^{2h} \dot{E}_{aph} \quad b \dot{E}_{bnh} = a^h \dot{E}_{aph} \quad (3)$$

$$c \dot{E}_{cph} = a^h \dot{E}_{aph} \quad c \dot{E}_{cnh} = a^{2h} \dot{E}_{anh} \quad (4)$$

with h , b and c being respectively the harmonic order and real numbers and $a = e^{j(2\pi/3)}$.

With \dot{Z}_{aph} and \dot{Z}_{anh} being the positive and negative sequence impedance relative to the order h space

harmonic, the result of a parallel association of the magnetization reactance with the corresponding secondary sequence impedance referred to the same harmonic order. Taking into consideration the *phase A* as the reference, the *emf* can be related with currents through equations (5) and (6).

$$\dot{E}_{aph} = \dot{Z}_{aph} \dot{I}_{aph} \quad (5) \quad \dot{E}_{anh} = \dot{Z}_{anh} \dot{I}_{anh} \quad (6)$$

Where \dot{I}_{aph} and \dot{I}_{anh} are asymmetric positive and negative sequence components respectively. These components are related to the feeding currents in the phases of the primary winding, which in turn make possible the following equalities:

$$\dot{I}_{ap1} = \dot{I}_{an5} = \dot{I}_{ap7} = \dot{I}_{an11} = \dot{I}_{ap13} = \dots = \dot{I}_{ap} \quad (7)$$

$$\dot{I}_{an1} = \dot{I}_{ap5} = \dot{I}_{an7} = \dot{I}_{ap11} = \dot{I}_{an13} = \dots = \dot{I}_{an} \quad (8)$$

where the numeric indexes are the harmonic orders.

Equations (5) and (6) and relationships (7) and (8) allows the drawing of the positive and negative sequence series equivalent circuits[3].

Based in the circuit mentioned above the following expressions are extracted:

$$\dot{E}_{ap} = \dot{E}_{ap1} + \dot{E}_{an5} + \dot{E}_{ap7} + \dot{E}_{an11} + \dots \quad (9)$$

$$\dot{E}_{an} = \dot{E}_{an1} + \dot{E}_{ap5} + \dot{E}_{an7} + \dot{E}_{ap11} + \dots \quad (10)$$

with

$$\dot{E}_a = \dot{E}_{ap} + \dot{E}_{an} \quad (11)$$

and

$$\dot{E}_b = \dot{E}_{bp} + \dot{E}_{bn} \quad (12)$$

$$\dot{E}_c = \dot{E}_{cp} + \dot{E}_{cn} \quad (13)$$

$$\dot{E}_{ap} = \dot{I}_{ap} (\dot{Z}_{ap1} + \dot{Z}_{an5} + \dot{Z}_{ap7} + \dot{Z}_{an11} + \dots) \quad (14)$$

$$\dot{E}_{an} = \dot{I}_{an} (\dot{Z}_{an1} + \dot{Z}_{ap5} + \dot{Z}_{an7} + \dot{Z}_{ap11} + \dots) \quad (15)$$

$$\dot{Z}_{ap} = \dot{Z}_{ap1} + \dot{Z}_{an5} + \dot{Z}_{ap7} + \dot{Z}_{an11} + \dots \quad (16)$$

$$\dot{Z}_{an} = \dot{Z}_{an1} + \dot{Z}_{ap5} + \dot{Z}_{an7} + \dot{Z}_{ap11} + \dots \quad (17)$$

With some algebraic manipulation can be obtained:

$$\begin{bmatrix} \dot{V}_a \\ \dot{V}_b \\ \dot{V}_c \end{bmatrix} = \begin{bmatrix} \dot{Z}_a 1 + f_d & \dot{Z}_{ap} & \dot{Z}_{an} \\ \dot{Z}_b a^2 + af_d & \frac{a^2}{b} \dot{Z}_{ap} & \frac{a}{b} \dot{Z}_{an} \\ \dot{Z}_c a + a^2 f_d & \frac{a}{c} \dot{Z}_{ap} & \frac{a^2}{c} \dot{Z}_{an} \end{bmatrix} \begin{bmatrix} \dot{I}_{a1} \\ \dot{I}_{ap} \\ \dot{I}_{an} \end{bmatrix} \quad (18)$$



Figure 1 – Linear induction motor: 1 – primary package, 2 – secondary in an aluminum disc.

The active power transferred to the secondary through the air-gap, referred to the order *h* space harmonic are given as follows:

$$P_{ph} = 3 I_{aph}^2 \Re_e(\dot{Z}_{aph}) \quad (19)$$

$$P_{nh} = 3 I_{anh}^2 \Re_e(\dot{Z}_{anh}) \quad (20)$$

$$v_{sdh} = \frac{v_{sx}}{h} \quad (21)$$

where v_{sx} being the linear synchronous speed.

The developed positive (F_{uph}), negative (F_{unh}) sequence and resulting (F_u) thrust are given by:

$$F_{uph} = \frac{P_{ph}}{v_{sxh}} ; \quad F_{unh} = -\frac{P_{nh}}{v_{sxh}} \quad (22)$$

$$F_u = \sum_h (F_{uph} + F_{unh}) \quad (23)$$

III. PROTOTYPE

In this work, a three-phase, two pole, two-sided with short primary LIM, was built and tested in the Electrical Machines Laboratory. The primary stacks (stator) are made of steel silicon sheets (core) and the secondary (linor) constituted of a non-ferromagnetic material, the aluminum, with the shape of a flat disc, which illustrated in Figure 1.

The primary winding in each stack is made of copper, three-phase, concentric type, set of steps 1:8 and 2:7, one layer, 200 turns in each phase with coil scheme shown in Figure 2.

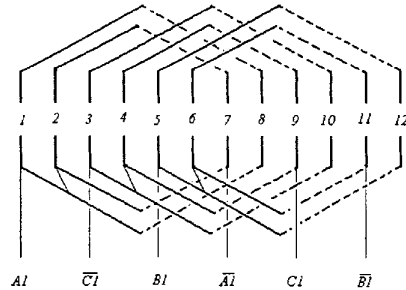


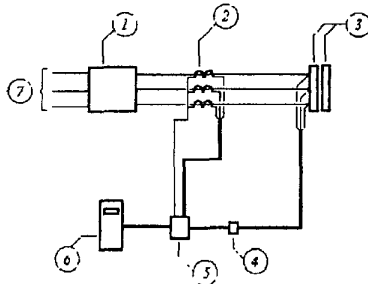
Figure 2 – Winding scheme for each primary package.

The architecture of primary packages has finite length, the primary winding is spread along the direction of movement, the secondary structure is a solid aluminum disc. The relative movement between primary and secondary is the cause of interesting phenomena called *end effects*, and also the unbalance in phase voltage and currents. End effects are mainly caused by the opened structure of a LIM, regarding its magnetic circuit, when compared with the closed structure of an ordinary three-phase induction motor[4][5][6]. In this sense the opened structure is the cause of unbalance in phase voltages and currents.

IV. TESTS AND EXPERIMENTAL RESULTS

The first step to obtain the LIM parameters is to get experimentally the stator leakage inductance following the procedures from reference [1].

The primary phases resistances are obtained through direct measurements. The magnetization reactance is obtained from no-load tests; this test can be made without a linor or with a moving linor at synchronous linear speed. Determination of secondary impedance is made with a locked linor. In both cases the experimental procedure follows the scheme in Figure 3.



Specifications.
AC Power Source /analyzer
Frequency: 45/1000 Hz;
Voltage: 0 – 300V;
Power: 4.5 KVA;
Current Hall effect sensor.
Set of two blocks defining the stator;
Voltage Hall effect sensor.
Data acquisition system;
Personal Computer CPU;
Feeding from the mains.

Figure 3 - Laboratory scheme to obtain voltage and current waveforms.

The current signal is obtained through the application to the machine of a sinusoidal three-phase balanced voltage system, with a data acquisition system the voltage and current waveforms referred to each test were obtained. In the appendix are presented figures illustrating the voltage and current waveforms obtained in no load and linor locked tests.

Voltage and current waveforms obtained have time harmonics of high order. Therefore, the use of Fast Fourier Transform (FFT) allow the acquisition of harmonic content magnitude up to a certain order, which in our case, following international standards, is the 50th harmonic. It will be possible then, to obtain the Total Harmonic Distortion (THD). A data acquisition system is used to get the feeding voltage and current for each test. Since the THD in time for voltage and current is always lower than 0.5%. Only first harmonic time components are considered in this case. Therefore, it is obtained, the correspondent complex values for voltage and current waveforms. The mathematical development presented previously allow us to obtain the parameter values considering only the space harmonics up to the 11th order.

No-load data test(rms values):

Table 1 - Percentile values relative to the fundamental component of harmonic content up to the 7th order

-----	V _a	V _b	V _c	I _a	I _b	I _c
Fund	100	100	100	100	100	100
2 nd	0.0701	0.0594	0.0958	0.0293	0.0126	0.0543
3 rd	0.1430	0.0505	0.0447	0.0599	0.0342	0.0278
4 th	0.0324	0.0213	0.0296	0.0049	0.0034	0.0211
5 th	0.0337	0.0229	0.0642	0.0094	0.0145	0.0185
6 th	0.0590	0.0049	0.0446	0.0153	0.0032	0.0336
7 th	0.0072	0.0166	0.0181	0.0255	0.0257	0.0113

Feeding at balanced line voltage (V) – V_L = 77.0171

Resulting values:

Phase voltages (V):

V_a = 46,9678, V_b = 46.6967, V_c = 39.9741

Phase currents (A):

I_a = 1.4900, I_b = 1.5297, I_c = 0.9897

Locked rotor data test(rms values):

Table 2 illustrate percentile values of harmonic content up to 7th order related to the fundamental component.

Table 2 - Percentile values relative to the fundamental component of harmonic content up to the 7th order

-----	V _a	V _b	V _c	I _a	I _b	I _c
Fund	100	100	100	100	100	100
2 nd	0.0616	0.0240	0.0470	0.0589	0.0285	0.0332
3 rd	0.1680	0.1443	0.0758	0.1042	0.0755	0.0640
4 th	0.0868	0.0424	0.0535	0.0458	0.0244	0.0279
5 th	0.1004	0.0701	0.1164	0.0288	0.0190	0.0586
6 th	0.1288	0.0407	0.0779	0.0467	0.0201	0.0431
7 th	0.0141	0.0412	0.0066	0.0296	0.0119	0.0380

Feeding at balanced line voltage (V) – V_L = 75.6990

Resulting values:

Phase voltages (V):

V_a = 45.0288, V_b = 45.3695, V_c = 40.7952

Phase currents (A):

I_a = 3.2980, I_b = 3.2923, I_c = 2.5687

The obtained parameters are illustrated in Table 3.

Table 3 – Values (Ohm) of the experimentally obtained LIM parameters.

PHASE	IMPEDANCE		MAGNETIZATION REACTANCE
	PRIMARY	SECONDARY	
A	5.3479 + j5.7290	13.1006 + j1.0597	39.9030

V. THEORETICAL AND EXPERIMENTAL VALIDATION

With a locked linor, the developed thrust and *rms* current will them be measured for different applied *rms* voltage values. With the measured voltage values the current and thrust will be consequently calculated and estimated the percentage difference between measured and calculated values. Table 4 shows the theoretical and experimental validation for the following line voltages: 45.0; 50.3; 51.6; 57.7; 61.6; 66.4; 70.0 and 75.7 Volts.

Table 4 has the values of measured (m) currents as base values, and percentage differences (dif) calculated for the fundamental space harmonics (dif1) and for all the space harmonics up to the 11th (dif11).

The following figure shows the measured and calculated thrust against line voltage with locked linor. The continuous line represents the experimental values (lab tests), the small trace line shows the calculated values when considered space harmonics up to the order 11th (Theory (1)) the bigger trace line shows the calculated values for the fundamental space harmonics (Theory(2)).

Table 4. Values (rms) for measured (m) currents (A), and percentage difference against measured values dif1 and difl1, referred to phases A, B and C.

Phase A		
Ia (m)	dif1	difl1
2.0252	3.5681	5.2531
2.2292	1.8431	3.7808
2.2888	0.6159	3.8790
2.5670	1.0612	4.1113
2.7115	0.6916	3.0069
2.9109	0.5280	2.6850
3.0914	1.0849	3.4127
3.2980	0.0036	2.0763

Phase B		
Ib (m)	dif1	difl1
2.0251	3.8742	4.4112
2.2271	2.0058	2.7887
2.2887	0.6896	2.9331
2.5642	1.2235	3.3367
2.7091	0.7697	2.0961
2.9073	0.5721	1.5968
3.0862	1.0838	2.4501
3.2923	0.0003	0.9640

Phase C		
Ic (m)	dif1	difl1
1.5805	4.0804	-0.3526
1.7394	2.0370	-1.9076
1.7857	0.7902	-1.7130
2.0016	1.2231	-1.5337
2.1159	0.8760	-2.6438
2.2691	0.6086	-2.9404
2.4110	1.2129	-2.1086
2.5687	0.0016	-3.5848

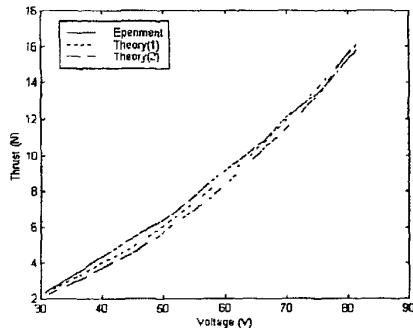


Figure 4 - Thrust against line voltage - linor locked condition.

This investigation allowed us to also measure the thrust against the linear speed, for different operating conditions. To make this measurement a direct current generator was connected to the axis of the secondary disc, with the generator feeding a bank of resistive loads. To achieve a reasonable accuracy in speed measurements a micro processed encoder with an active optical sensor was used. Theoretical and experimental results are presented in Figure 5, showing also that the method is entirely valid for a diversity of values of rotor slip. In this Figure 5 the stars are measured values (lab tests), the small trace line shows

the calculated values when considered space harmonics up to the order 11th (Theory (1)) the bigger trace line shows the calculated values for the fundamental space harmonics (Theory(2)).

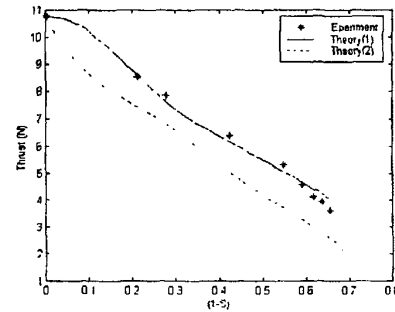


Figure 5 - Thrust against (1-S). S is the rotor slip, machine fed by a line voltage of 63.1892 Volts (rms).

VI. CONCLUSION

The idea of equivalence proved to be a good choice and also can be a tool to make easier future dynamic studies for the linear induction motor. With the given current tables it is easy to verify that the small percentage difference between measured and calculated current values validates the model. The method turned to be more effective when higher order space harmonics were introduced.

LIM current unbalance is caused not only by its architecture, but also by end effects.

In the case of thrust with a moving linor, we can easily conclude that the presented model has been validated for a wide range of operating speed conditions, mainly for speeds that can reach up to sixty percent of the synchronous linear speed.

This work shows a method to obtain LIM phase parameters through the process of obtaining voltage and currents at the machine terminals. The philosophy adopted along this research development is to implement new factors in the modeling. This first attempt, the inclusion of space harmonics showed up to be a good choice. A follow up to this stage will be the inclusion of new factors in the model, this will be the next step for a closer agreement between theoretical and practical results.

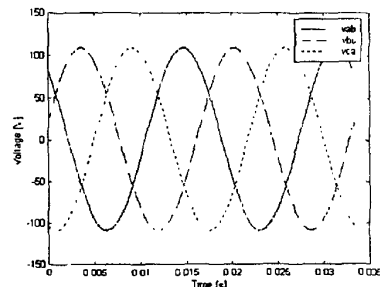


Figure 6 - Line voltages for a no load condition under an applied "rms" line voltage of 77.017 V.

VII. APPENDIX

As an illustration Figures 6, 7 and 8, show the line voltages, phase voltages and current waveforms respectively. Those results were obtained in one of the tests performed. This is a case of a no load condition under an applied "rms" line voltage of 77.017 V.

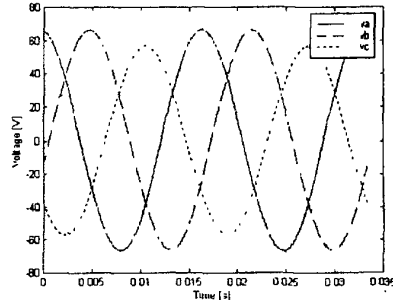


Figure 7 - Phase voltages for a locked linor under the same conditions as in Figure 6

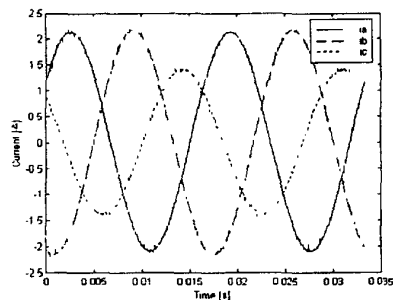


Figure 8 - Phase currents for a locked linor under the same conditions as in Figure 6.

Figures 9, 10 and 11, illustrate the line voltages, phase voltages and current waveforms respectively, referred to the other test with locked linor and the machine under feeding line voltage of 75.699 Volts (rms).

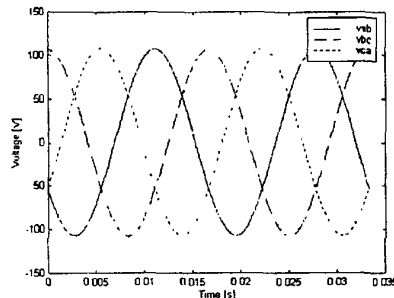


Figure 9 - Line voltages for a locked linor under an applied "rms" line voltage of 75.699 V.

VIII. BIOGRAPHY

Luciano Martins Neto - Dr. Martins Neto was born in Botucatu, SP, Brazil on May 22nd, 1948. He has a Doctoral degree in Mechanical Engineering from Escola de Engenharia de São Carlos at Universidade de São Paulo (USP), São Carlos, Brazil since 1980. Worked as a lecturer at Faculdade de Engenharia de Lins, Lins, SP, Brazil, at Escola de Engenharia de São Carlos (USP), São Carlos, Brazil and at the Electrical Engineering Department (UNESP - Universidade Estadual Paulista) at Ilha Solteira, SP, Brazil. He is currently working as a Senior Lecturer at

Universidade Federal de Uberlândia, MG, Brazil. His areas of interest are Electrical Machines and Grounding.

Euler B. dos Santos - Mr. Santos was born in Goiás, Goiás, Brazil. He got his BSc degrees in Electrical Engineering in 1977 and in Physical Sciences in 1979 from UFG - Universidade Federal de Goiás, Goiânia, Brazil. He is a lecturer at UFG since 1977. His MSc degree was obtained in 1993 from UFU - Universidade Federal de Uberlândia where he is currently pursuing his Doctoral degree. His areas of interest are Electrical Machines and Automation.

José Roberto Camacho - Dr. Camacho was born in Taquaritinga, SP, Brazil on November 3rd, 1954. Completed his PhD degree in the Electrical and Electronic Engineering Department at the University of Canterbury, Christchurch, New Zealand, in August 1993. He is a Senior Lecturer at Universidade Federal de Uberlândia where he works since February 1979. Dr. Camacho is a Researcher-Consultant of CNPq (Brazilian National Council for Scientific and Technological Development) and worked as a collaborator-member of Brazilian Committee of CIGRÉ-JWG 11/14-09 (Unit Connection). His areas of interest are Dynamic Simulation, Electrical Machines and HVAC-DC conversion.

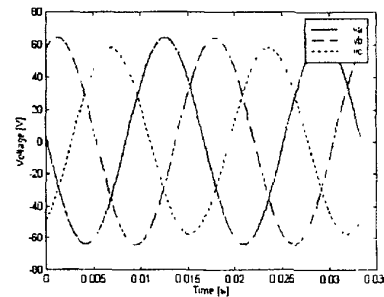


Figure 10 - Phase voltages for a locked linor under the same conditions as in Figure 9.

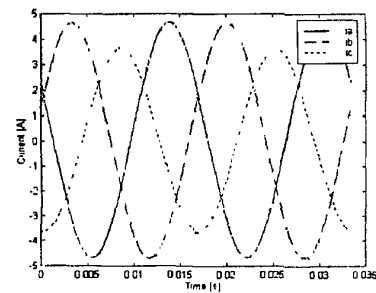


Figure 11 - Phase currents for a locked linor under the same conditions as in Figure 9.

IX. REFERENCES

- [1] MARTINS NETO, L. e SANTOS, E.B. (1998). Linear Induction Motor Inductance Determination Method - (In Portuguese) - XII CBA, Uberlândia, MG, Brazil.
- [2] STEVENSON JR., W. D., (1982). Elements of Power System Analysis, Fourth Edition, McGraw-Hill, New York.
- [3] GIERAS, J.F. (1994). Linear Induction Drivers, Clarendon Press, Oxford.
- [4] YAMAMURA, S. (1978). Theory of Linear Induction Motors, University of Tokyo Press.
- [5] BOLDEA I. and NASAR S. A. (1985). Linear Motion Electromagnetic Systems, John Wiley & Sons, New York.
- [6] SIMONE, G. A. (1992). Double Face Linear Asynchronous Converters - Theory and Design, Doctoral Thesis (In Portuguese), FEE - UNICAMP, Campinas, SP, Brazil.
- [7] MARTINS NETO, L. (1980). Asymmetrical Three-Phase Induction Motor Phase Number Converter, Doctoral Thesis (In Portuguese), USP - São Carlos, Brazil.